



UNIVERSIDADE ESTADUAL DE CAMPINAS  
SISTEMA DE BIBLIOTECAS DA UNICAMP  
REPOSITÓRIO DA PRODUÇÃO CIENTÍFICA E INTELLECTUAL DA UNICAMP

**Versão do arquivo anexado / Version of attached file:**

Versão do Editor / Published Version

**Mais informações no site da editora / Further information on publisher's website:**

<https://journals.sagepub.com/doi/10.1177/0021998321999438>

**DOI: 10.1177/0021998321999438**

**Direitos autorais / Publisher's copyright statement:**

©2021 by Sage. All rights reserved.

DIRETORIA DE TRATAMENTO DA INFORMAÇÃO

Cidade Universitária Zeferino Vaz Barão Geraldo

CEP 13083-970 – Campinas SP

Fone: (19) 3521-6493

<http://www.repositorio.unicamp.br>

# Study of three distinct self-compacting concretes containing marble/granite powder and hooked-end steel fiber contents

Journal of Composite Materials  
2021, Vol. 55(20) 2823–2838  
© The Author(s) 2021  
Article reuse guidelines:  
sagepub.com/journals-permissions  
DOI: 10.1177/0021998321999438  
journals.sagepub.com/home/jcm



Beatriz C Xavier<sup>1</sup>, Amauri E Gomes<sup>2</sup>, Mirian LNM Melo<sup>2</sup> ,  
Rosa C Cecche Lintz<sup>1</sup>, Luísa A Gachet<sup>1</sup> and  
Wislei R Osório<sup>1,3</sup>

## Abstract

In this investigation distinctive self-compacting concretes (SCC) containing both marble + granite (MG) powder and hooked-end steel fibers (HESF) are investigated. A mixture of conventional SCC (reference), and other five samples containing MG and steel fiber (SF) contents are provided, *i.e.* 20MG, 20SF, 30MG + 10SF, 20SF and 30MG + 20 SF. Both the fresh and hardened properties of the modified self-compacting concretes are evaluated. Workability of the SCC samples represented by slump flow, L-box, V-funnel, J-ring and flowability  $T_{500}$  is examined. The properties of hardened state of the SCC samples at 7 and 28 days are also evaluated. Modulus of elasticity, water absorption, voids index (indicating porosity), and specific mass are attained. Comparisons among specific strengths and consumptions of cement per compressive strengths are also provided. The SCC/30MG/10SF sample has a specific strength  $\sim 50\%$  higher than the conventional SCC sample. When a ratio involving porosity per cement consumption per tensile strength is evaluated, the SCC/30MG/10SF sample has this ratio  $\sim 80\%$  higher than the SCC reference. Additionally, the best result of consumption of cement (CC) per compressive strength (CS) ( $1.28\times$  lower than the SCC reference) at 28 days is that of the SCC/30MG/10SF sample ( $5.03 \text{ kg/m}^3 \cdot \text{MPa}^{-1}$ ). This indicates that an environmentally friendly aspect associated with low relative cost, which is an important parameter to consider in future SCC mixture designing.

## Keywords

Fresh and hardened concrete properties, self-compacting concrete, steel fibers, porosity, mechanical behavior, interfacial transition zone

## Introduction

Investigations about self-compacting concretes (SCC) with stone powder are widely reported,<sup>1–6</sup> as well as, SCC with marble or SCC with steel fiber<sup>1,2</sup> is also studied. However, studies concatenating both marble + granite (MG) powder with hooked-end steel fibers (HESF) are scarce. Based on this, the intrinsic novelty and contribution in this present investigation concerns to fresh and hardened characteristics of modified SCC samples with MG and HESF contents. Both MG and HESF contents are varied. Samples containing only MG without steel fiber (SCC/20MG) and only containing steel fibers (SCC/20SF) are produced. Also, samples concatenating MG and HESF (*i.e.* SCC/30MG + 10SF and SCC/30MG + 20SF) are produced.

Additionally, models (Ryshkewitch and Schiller<sup>7</sup>) describing compressive and tensile strengths with porosity are also discussed. Another contribution provided concerns to a promise lower cement

<sup>1</sup>School of Technology, University of Campinas – UNICAMP, Brazil

<sup>2</sup>Institute of Mechanical Engineering, Federal University of Itajubá (IEM-UNIFEI), Brazil

<sup>3</sup>School of Applied Sciences/FCA, University of Campinas – UNICAMP, Brazil

### Corresponding author:

Wislei R Osório, School of Technology, University of Campinas – UNICAMP, Pedro Zaccaria St., Jd. Sta Luíza, Limeira, São Paulo 13484-350, Brazil.

Email: wislei1@unicamp.br

consumption, which induces that an environmentally friendly aspect associated with low relative cost is attained.

It is recognized that a SCC is characterized by its capable of flowing and consolidating when gravity and its weight are combined.<sup>3,4</sup> Consequently, the vacancies and spaces even in the presence of dense reinforcement can be efficiently filled. It has been reported that the waste materials have been reutilized in the civil construction sector.<sup>7–11</sup>

During the last 10 years, there exists a great number of SCC with marble contents.<sup>5,6,10–18</sup> It acts as filler<sup>12</sup> and a decrease in the total void content is provided.<sup>5,12–14</sup> It was also reported that a higher water/cement ratio than a conventional concrete is required, and consequently, a decrease in the compressive strength is reached.<sup>12–14</sup> The workability in the fresh state of a SCC is also improved when up to 10% marble content replaces the cement.<sup>5,15,16</sup> This indicates that environmentally friendly with an economical viable aspect seems to be associated.

Considering the steel fiber-reinforced SCC, the fiber addition is utilized in order to improve the resulting mechanical properties. However, the presence of fibers can potentially undermine the fresh-state properties and, consequently, the intrinsic characteristics of a SCC can be minimized.<sup>19</sup> Peng Zhang and collaborators<sup>20–22</sup> have recently reported distinct studies concerning to SCC with different fibers.

Investigations concern to the self-compacting concrete containing glass fibers and polypropylene fibers are also reported.<sup>21,23,24</sup> There exists a consensus that the controlling the use of fibers, the flexural strength and split tensile strength are improved.<sup>20–28</sup> Also, it is agreed that the total volume, size and its spatial dispersion have important roles on the performance of the concrete specimen.<sup>25–28</sup>

The use of the hooked-end steel fiber in different geometry (*i.e.* 3D, 4D and 5D) designated as Dramix® has been widely reported.<sup>29–31</sup> Ghasemi et al.<sup>29</sup> have reported the effects of distinct steel fiber proportions in a SCC (*i.e.* 0.1, 0.3 and 0.5% corresponding with 7.8, 23.5, and 39 kg/m<sup>3</sup>). From this mentioned study,<sup>29</sup> when a w/c of 0.52 and fiber contents of 0.3 to 0.5%, the flexural strength is increased. It is also concluded that energy absorption (represented by factor  $K_{IC}$ ) is decreased due to less space for rotation of fiber is provided. On the other hand, when the fiber content is increased, the fracture energy is increased and the SCC specimens exhibit ductile behavior.<sup>29</sup>

A SCC flows under its own weight without settlement, segregation, or bleeding, and filling the remote corners.<sup>32</sup> Since steel fibers (SF) constitute steel fiber reinforced-SCC (particularly using hooked-end steel fibers, HESF), superplasticizer as viscosity modifier

agent is commonly applied.<sup>11,19,29–32</sup> Also, other supplementary cementitious materials are used (*e.g.* fly ash and natural pozzolan contents, etc.).<sup>32</sup> With this, the water/binder ratio is decreased, and the viscosity is increased.

Based on the previous studies, the concatenated effects of marble/granite waste content and hooked-end steel fibers in a SCC are not investigated. With this, the novelty and contribution provided in this present investigation concerns the evaluation of these effects on both fresh and hardened-states of the modified SCC samples.

For this purpose, as aforementioned, samples of conventional and with only MG contents are produced and investigated. Also, sample containing only steel fibers are examined. Additionally, other samples concatenating both MG and HESF are also produced and examined. When both MG and HESF are used, the effects of the sand content ( $\sim 0.2\%$ ) replacing with MG content are also analyzed. These adopted concrete (SCC) mixtures are based on those previously investigations,<sup>11,29</sup> which is suggested a range of the w/c between 0.55 and 0.6 and a coarse aggregate using gravel #0.<sup>11,29</sup> With these proposed mixes, lower cement consumption is induced, and both mechanical behavior and economical aspects are also considered.

## Experimental procedure

### Materials

In order to verify the effects of both MG and fiber contents in SCC specimens, six different mixtures are produced. For this purpose, a high early strength (HES) Portland cement is used (according ASTM C150, NBN EN 197–1<sup>11</sup>). This kind of cement is adopted based on the fact that it has finer characteristic than other cements. With this, a more rapid hydration is provided, and a better hardened-state property during 7 days is reached. The specific mass and unit mass of the cement are 3.12 g/cm<sup>3</sup> and 1.03 g/cm<sup>3</sup>, respectively. Additionally, their initial and final setting times are 170 and 240 minutes (ABNT NBR 16607:2017), respectively. Also, their compressive strengths for 1, 3, 7 and 28 days are 27.5, 42.3, 46.8 and 56 MPa, respectively (ABNT NBR 7215:1997).

A natural quartzite sand as fine aggregate is used. It possesses a specific mass and fineness index of 2.65 g/cm<sup>3</sup> and 1.8, respectively. Their accumulative percentage of  $\sim 60\%$  is lower than 0.3 mm. Coarse aggregate as gravel #0 (from basaltic origin) is utilized. The adopted coarse aggregate (gravel #0) has specific mass and fineness index of 3.01 g/cm<sup>3</sup> and 3.9, respectively. Their corresponding size is ranged between 4.75 and 9.5 mm. This selection is also adopted from

previous investigations,<sup>11,29</sup> which have demonstrated that using a w/c ratio close to 0.52, the mechanical properties are satisfactorily reached.

The marble/granite (MG) powder content is supplied from an ornamental stone industry (located at Limeira, SP, Brazil). This material is collected in the sludge-shape, originated from the cutting and polishing processes.<sup>11</sup> The MG proportions at  $100 (\pm 5) ^\circ\text{C}$  during 24 hours are dried. A 0.6 mm mesh sieve is used in order to the MG content be derailed and sifted. The MG used has a specific mass of  $2.58 \text{ g/cm}^3$  and fineness index of 10.3. More characteristics concerning to MG are previously reported.<sup>11</sup> The x-ray diffraction patterns previously reported<sup>11</sup> indicate that phases corresponding with quartz (silica,  $\text{SiO}_2$ ), illite ( $\text{K(AlSi}_3\text{O}_8)$ ), kaolinite ( $\text{Al}_2\text{Si}_2\text{O}_5(\text{OH})_4$ ) and periclase ( $\text{MgO}$ ) are clearly identified.

When the SCC samples are added with silica fume, this material has a specific mass of  $2.21 \text{ g/cm}^3$  with  $\text{SiO}_2$  higher than 85% and morphology majority in spherical shape. It is incorporated to increase the cohesion of the mixture concrete and to decrease the porous induced when cement hydration is preceded.

A Dramix® 3 D HESF designated as Dramix RC65/35B<sup>19,30–32</sup> with density of  $7.85 \text{ g/cm}^3$  and ultimate tensile strength of about 1100 MPa is used, as shown in Figure 1. These characteristics are complied with ASTM A820.<sup>33</sup> This nomenclature identifies their length and diameter of about 35 mm and 0.55 mm, respectively. Although are commonly commercialized other dimensions and geometry, based on the previous investigation provided by Alberti et al.<sup>19</sup> and a possible limitation in fresh state, the Dramix® 3 D is adopted.

An ether polycarboxylate superplasticizer additive is used to prepare each one of the proposed SCC mixtures. The superplasticizer has a specific mass of  $1.08 \text{ g/cm}^3$  and pH 7.7.<sup>11</sup> It is used in portions between 0.2 and 2 wt.% of total mass, as also previously reported.<sup>11,29</sup> Tables 1 and 2 demonstrate properties of finer and coarser aggregates and their granulometric numbers, respectively.

### The proposed SCC mixtures

It is worth noted that the six distinct SCC mixtures are proposed in order to demonstrate the effects of the MG content associated with the hooked-end steel fibers (HESF) in both the fresh and hardened-states of the SCC samples examined. Besides, it is also remarked that the groups of the SCC mixtures are planned based on the fact that some variable parameters have previously been reported and elucidated.<sup>11,29</sup> With this, the variables such as w/c ratio, the kind of cement, coarse aggregate (gravel #0), hooked-end steel fibers (HESF) content are parameterized. The w/c ratios are

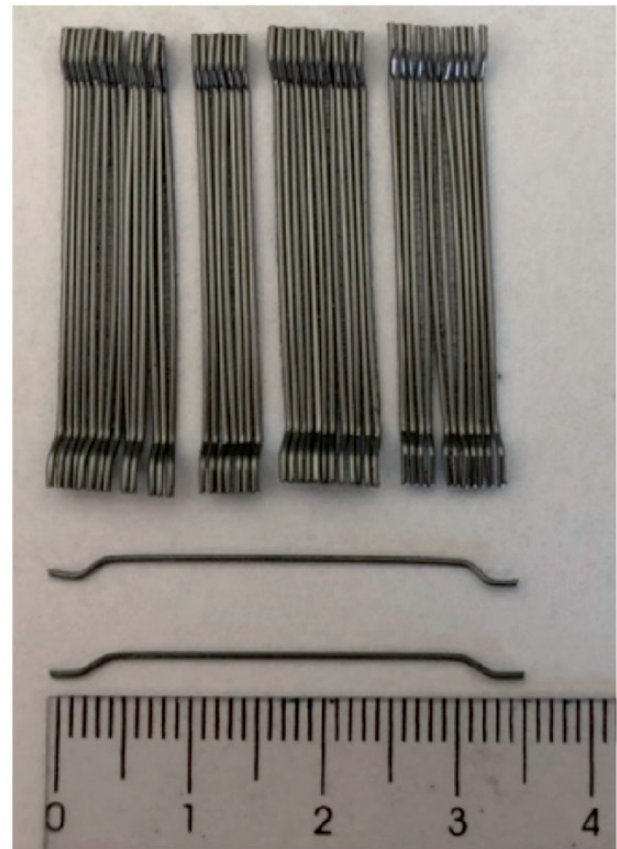


**Figure 1.** Typical Dramix® steel fiber constituting the hooked-end steel fibers (HESF) used as reinforcing in a SCC samples.

0.54 and 0.58 considering SCC with MG content and SCC with MG + HESF, respectively. Two distinct consumptions of fibers are adopted, *i.e.* 10 and  $20 \text{ kg/m}^3$ . Based on the previously reported studies,<sup>29–32</sup> there exists a great difficult to compare results of the fresh state of the SCC mixtures. Majority slump flow or V-funnel and other techniques are commonly used to characterize SCC fresh behavior.<sup>30–32</sup> Since fiber addition induces to certain decrease in the fresh state of a SCC, limitations are correlated with other parameter applied, as described by Alberti et al.<sup>19</sup> Based on these assertions, the aforementioned fiber consumptions are adopted.

Ananda et al.<sup>31</sup> have indicated the recommendations of the maximum dosages of the Dramix® steel fibers according with standard fabrication. It is indicated that a maximum aggregate up to 6 cm, the maximum dosages of 60 and  $45 \text{ kg/m}^3$  when pour and pump feed are considered, respectively.<sup>31</sup> In this present investigation, the adopted dosage of Dramix® fibers are 10 and  $20 \text{ kg/m}^3$ , which are similar to those previously reported by Ghasemi et al.<sup>29</sup> It is also remarked that w/c ratio and coarse aggregate are similar to those utilized by Ghasemi et al.<sup>29</sup>



**Table 1.** The proposed mix proportions of the SCC samples with distinctive MG powder content and Dramix® steel fibers (SF).

Mix	Cement (kg/m <sup>3</sup> )	Silica fume (kg/m <sup>3</sup> ) (mass)	SF (kg/m <sup>3</sup> ) (mass)	MG (kg/m <sup>3</sup> ) (mass)	Coarse aggregate (kg/m <sup>3</sup> ) (mass)	Sand (kg/m <sup>3</sup> ) (mass)	Water (kg/m <sup>3</sup> )	Superplasticizer (%)
SCC	379	0	0	0	789 2.8	1073 2.83	205	1
SCC/20MG	368	0	0	74 <sup>b</sup> 0.2	766 2.8	1042 2.83	199	1
SCC/10SF	367	36.7 0.10	10 0.026	0	764 2.8	1039 2.83	212	2
SCC/30MG/10SF	367	36.7 0.10	10 0.026	110 <sup>a</sup> 0.30	764 2.8	925 2.52	212	2
SCC/0MG/20SF	366	36.6 0.10	20 0.052	0	762 2.8	1036 2.83	212	2
SCC/30MG/20SF	351	35.1 0.10	20 0.052	105 <sup>b</sup> 0.30	730 2.8	994 2.52	204	2

<sup>a</sup>Proportion is replaced with the sand weight.

<sup>b</sup>Proportion is added to SCC.

**Table 2.** Experimental fresh state results of the slump flow L-box, V-funnel, J-ring, and flowability time  $T_{500}$  of the examined SCC and modified SCC samples.

Mixtures	Slump flow (mm)	Class	L-Box	V Funnel (s)	Class	J-Ring (mm)	Class	$T_{500}$	Class
SCC	710	SF 2	<b>0.63</b>	3.1	VF I	50	PJ I	1.2	VS I
SCC/20MG	740	SF 2	<b>0.88</b>	3.1	VF I	0	PJ I	1.3	VS I
SCC/10SF	730	SF 2	<b>0.80</b>	3.1	VF I	20.00	PJ I	1.1	VS I
SCC/30MG/10SF	838	SF 3	<b>0.90</b>	3.2	VF I	25.00	PJ I	1.9	VS I
SCC/0MG/20SF	735	SF 2	<b>0.63</b>	8.0	VF I	17.50	PJ I	1.0	VS I
SCC/30MG/20SF	725	SF 2	<b>0.74</b>	4.1	VF I	15.75	PJ I	2.0	VS I

The mixture proportions utilized to constitute the proposed SCC samples are shown in Table 1. In order to guarantee the reproducibility and to determine the compressive strength, for each one the proposed mixtures, at least 10 specimens are molded. The proportions of the materials selected are included into an electrical concrete mixer (capacity of 120 L) in the follow sequence: coarse aggregate with 2/3 of total water volume; cement, MG and sand contents. The remained water volume is added with superplasticizer additive. The forming is carried out with concrete mixtures being poured inside a metallic mold. After 24 h, the specimens are demolded and humidity curing at 23 ( $\pm 2$ ) °C with air relative humidity level higher 95% is preceded.

It is remarked that the pouring and forming methods to constitute SCC mixtures with MG and HESF are similar when conventional SCC is preceded. A more cohesion of mixture is attained when MG content is used.<sup>11</sup> It is known that a drawback of SCC is no cohesion in cement paste and, consequently, coarse aggregates are heterogeneously segregated. A decrease

in segregation of coarse aggregates is reached when fine aggregate is used.<sup>11</sup> Based on aforementioned fresh properties (workability aspects), it is also believed that in practical application both pouring and forming are also similar to a conventional SCC. Additionally, when MG content is used, the cohesion of mixture is increased and HESF or steel fiber segregation is decreased. To determine the Young's moduli of the distinct proposed samples, 06 specimens are elaborated.

### Fresh and hardened properties

The fresh state properties of the distinct SCC samples are determined using a Brazilian standard ABNT NBR 15,823: 2017, which has international equivalence standard. According with ASTM C1611-18, the traditional slump flow measurements are carried out. The measurement of both the "L-box" and "V-funnel" techniques are also provided (ABNT NBR 15823:2017 similar to JIS A 1115, A 1138, and BS EN 12350-9). These procedures are carried out in order to measure

**Table 3.** Experimental results of hardened state of the distinct SCC samples at 7 and 28 days.

Sample	Compressive strength, CS (MPa)		Tensile strength, TS (MPa)	
	7 days	28 days	7 days	28 days
SCC	49 ( $\pm 2$ )	59 ( $\pm 2$ )	4.5 ( $\pm 0.5$ )	4.8 ( $\pm 0.5$ )
SCC/20MG	50 ( $\pm 2$ )	61 ( $\pm 2$ )	4.7 ( $\pm 0.5$ )	5.0 ( $\pm 0.5$ )
SCC/10SF	58 ( $\pm 2$ )	73 ( $\pm 2$ )	5.7 ( $\pm 0.5$ )	6.4 ( $\pm 0.5$ )
SCC/30MG/10SF	57 ( $\pm 2$ )	73 ( $\pm 2$ )	5.8 ( $\pm 0.5$ )	6.8 ( $\pm 0.5$ )
SCC/0MG/20SF	50 ( $\pm 2$ )	71 ( $\pm 2$ )	6.0 ( $\pm 0.5$ )	6.2 ( $\pm 0.5$ )
SCC/30MG/20SF	55 ( $\pm 2$ )	73 ( $\pm 2$ )	5.5 ( $\pm 0.5$ )	7.3 ( $\pm 0.5$ )

the ability of the concrete to pass through obstacles, and to flow under certain conditions.<sup>11</sup>

The hardened behavior of the proposed SCC samples is represented by the compressive strengths, following procedures described into ABNT NBR 5739:2007.<sup>34</sup> For this purpose, a loading speed of about 0.45( $\pm 0.15$ ) MPa/s is adopted. The elasticity moduli of the SCC samples are determined using the static method (conventional compression method) according to ABNT NBR 7222:2011.<sup>35</sup> Additionally, the moduli of elasticity of the proposed SCC samples are also determined using the IET (impulse excitation technique), which is a dynamic non-destructive method, and their procedures are described in ASTM C215-14<sup>36</sup> and ASTM E1876-15<sup>37</sup> standards. A Sonelastic® equipment<sup>38</sup> to carry out the IET experimentations is utilized.

## Results and discussion

### Fresh state of the examined SCC samples

From the point of view of the fresh state behavior of a SCC specimen, a high workability or flowability is intrinsically demanded. Table 2 shows the experimental results of the slump flow, L-box, V-funnel, J-ring and flowability time  $T_{500}$  of the conventional SCC and the modified SCC samples examined. Considering the spreading results reached for all SCC examined, except the SCC/30MG/10SF classified as SF 3, the classification SF 2 corresponds with all other SCC samples examined. Although the obtained results of L-box of the SCC and the SCC/0MG/20SF are slightly lower than those attained by method L-box (*i.e.* the value should be  $\geq$  than 0.80), all other samples have their corresponding fresh state parameters indicating a satisfactory SCC behavior (acceptable workability). Although all other parameters demonstrate satisfactory workability, the results of the L-box corresponding with the SCC and SCC/0MG/20SF have pointed out certain attention.

Interestingly, the L-box result of the SCC sample is improved, *i.e.* it has increased from 0.63 to 0.88. Remembering that the parameter should be higher than 0.8, as described in ABNT NBR 15823-1:2017. Similarly, in another side of Table 2, the SCC/0MG/20SF sample reveals 0.63 as their corresponding L-box result. It is remembered that this mixture sample no contains MG content. It is recognized that SF addition can decrease the workability. However, it is suggested that the absence of MG content corroborates with the decrease in the L-box parameter. Besides, when the SCC/20MG reveals its L-box result increased when compared with the SCC, it is also induced that the MG content improves the results of fresh state of the SCC mixture. Again, it is remarked that all other investigated fresh state parameters have indicated a satisfactory workability, as depicted in Table 2.

The V-funnel method indicates an apparent plastic viscosity. It indicates that all examined SCC samples are classified as VF 1 (*i.e.* when value is < than 9 s). Besides, J-ring and the parameter  $T_{500}$  (ABNT NBR 15823-1:2017) are also indicating satisfactory workability, which are classified as PJ1 and VS1, respectively. These fresh state results are similar to those previously published,<sup>5,11,29</sup> which are similar in terms of the w/c ratio, marble and fiber contents and type of cement utilized. However, it is worth noted that a modified SCC containing HESF+MG has not previously reported. Since the fresh states of the proposed SCC mixture samples are satisfactory, their corresponding hardened properties during 7 and 28 days are determined.

### Hardened properties of examined SCC samples

The curing periods of 7 and 28 days are adopted. The first corresponds with that, when a HES cement is utilized. The period of 28 days corresponds with a common period reported in literature and comparison is facilitated. Since the hardened state parameters at 7 days are according with expected when a HES is used, it is considered that 28 days corresponding with

**Table 4.** Experimental results of the moduli of elasticity (E) determined by static (Es) and dynamic (Ed) using IET of the examined SCC samples at 7 and 28 days.

Sample	Es (GPa)		Ed (GPa)	
	7 days	28 days	7 days	28 days
SCC	36.5 ( $\pm 0.5$ )	41.0 ( $\pm 0.5$ )	n/a	n/a
SCC/20MG	40.0 ( $\pm 0.5$ )	40.6 ( $\pm 0.5$ )	n/a	n/a
SCC/10SF	34.5 ( $\pm 0.5$ )	39.8 ( $\pm 0.5$ )	41.7 ( $\pm 0.5$ )	44.4 ( $\pm 0.5$ )
SCC/30MG/10SF	36.3 ( $\pm 0.5$ )	40.2 ( $\pm 0.5$ )	42.3 ( $\pm 0.5$ )	45.6 ( $\pm 0.5$ )
SCC/0MG/20SF	36.2 ( $\pm 0.5$ )	40.7 ( $\pm 0.5$ )	n/a	45.5 ( $\pm 0.5$ )
SCC/30MG/20SF	37.0 ( $\pm 0.5$ )	40.1 ( $\pm 0.5$ )	n/a	45.9 ( $\pm 0.5$ )

n/a = not available.

a period age sufficient to prescribe the mechanical behavior trends. The experimental results of the hardened state obtained by using compressive strength (CS) and tensile strength (TS) are shown in Table 3.

As expected, all examined SCC samples have CS values at 28 days higher than the values corresponding with the period of 7 days. However, it is remarked that at 7 days, all examined SCC samples have reached at least a CS value of 49 MPa, which is expected when HES cement is used. According to ASTM C150, NBN EN 197-1,<sup>11,39</sup> at 7 days of curing, a minimum CS of 42.5 MPa (CEM-I 42.5) for HES cement is recommended. At 7 days, comparing with other cement, this has a more rapid hydration and higher cohesion than the conventional (ordinary Portland) cement.<sup>39,40</sup>

Although in recent study of Ghasemi et al.,<sup>29</sup> a Portland cement type II is used, similar characteristics of the main contents are observed (*i.e.*  $\sim 63\%$  CaO,  $\sim 21\%$  SiO<sub>2</sub>,  $\sim 5\%$  Al<sub>2</sub>O<sub>3</sub>,  $\sim 3.5\%$  Fe<sub>2</sub>O<sub>3</sub>,  $\sim 2\%$  SO<sub>3</sub>,  $\sim 7\%$  C<sub>3</sub>A and other). The HES used in this present investigation has the composition containing: 63.3% CaO, 19.2% SiO<sub>2</sub>, 5.2% Al<sub>2</sub>O<sub>3</sub>, 2.8% Fe<sub>2</sub>O<sub>3</sub>, 2.8% SO<sub>3</sub>, and 7.8% C<sub>3</sub>A and other, as previously reported.<sup>11,39,40</sup>

Although it is known that comparisons among distinct SCC mixtures are difficult to be made, the CS and TS values reported by Ghasemi et al.<sup>29</sup> are compared. They<sup>29</sup> have proposed a steel fiber consumption of 7.8 kg/m<sup>3</sup> (using Dramix® 3D) associated with a 0.52 w/c ratio. They have obtained CS, TS and E (modulus of elasticity) of about 49 MPa, 3.5 ( $\pm 0.3$ ) MPa and 28 ( $\pm 2$ ) GPa, respectively. Considering this present study, at 7 days using a HESF consumption of 10 kg/m<sup>3</sup> (designated as SCC/10SF) and a w/c ratio of 0.58, the corresponding CS, TS and E values are 50 ( $\pm 2$ ) MPa, 5 ( $\pm 0.5$ ) MPa; and 34.5 ( $\pm 0.5$ ) and 41.7 ( $\pm 0.5$ ) GPa (using static and IET methods), respectively. These moduli values are shown in Table 4 and forwardly are discussed.

Considering the effect of the HESF in the SCC samples, it is observed that at 7 and 28 days, the CS of the SCC/10SF sample is of about 20% higher than the SCC sample. Similar improvement is also obtained when the TS results are analyzed. This indicates that the SCC/10SF sample at 28 days has its mechanical behavior at least 85% higher than the SCC sample.

Literature indicates that MG content has no significant modification in mechanical behavior.<sup>5,6,11,12,14,16,18</sup> Additionally, it is previously reported SCC with three distinct MG content and no substantial ( $\sim 52$  MPa at 28 days) effects are verified.<sup>11</sup> However, a reasonably positive (improvement) effect on the fresh state results is attained, mainly that corresponding with L-box results. The SCC/30MG/10SF sample has no substantial improvements when the SCC/10SF sample is compared. Additionally, when the double HESF content is considered, no substantial improvements in both the compressive and flexural characteristics are also observed (considering 28 days). This observation is also validated when the MG content is adopted, *i.e.* the same order of magnitude of both the CS and TS results are reached. This means that the SCC/30MG/10SF and SCC/10SF samples have shown the best results in terms of the mechanical behavior. On the other hand, when the workability results (mainly L-box) are considered, the best L-box results concatenating the CS and TS values is revealed for the SCC/30MG/10SF sample.

When the moduli results using the static (destructive) method are analyzed, it is elucidated that, similar Es results are attained (considering 28 days). Similar conclusion is also provided when the Ed values are determined. However, the non-destructive method (IET) indicates Ed values slightly higher (up to 15%) than the Es results, as shown in Table 4. This seems to be associated with the IET utilized, as previously reported.<sup>41-43</sup> Lord and Morrel<sup>42</sup> have reported that uncertainty in the modulus is undoubtedly a

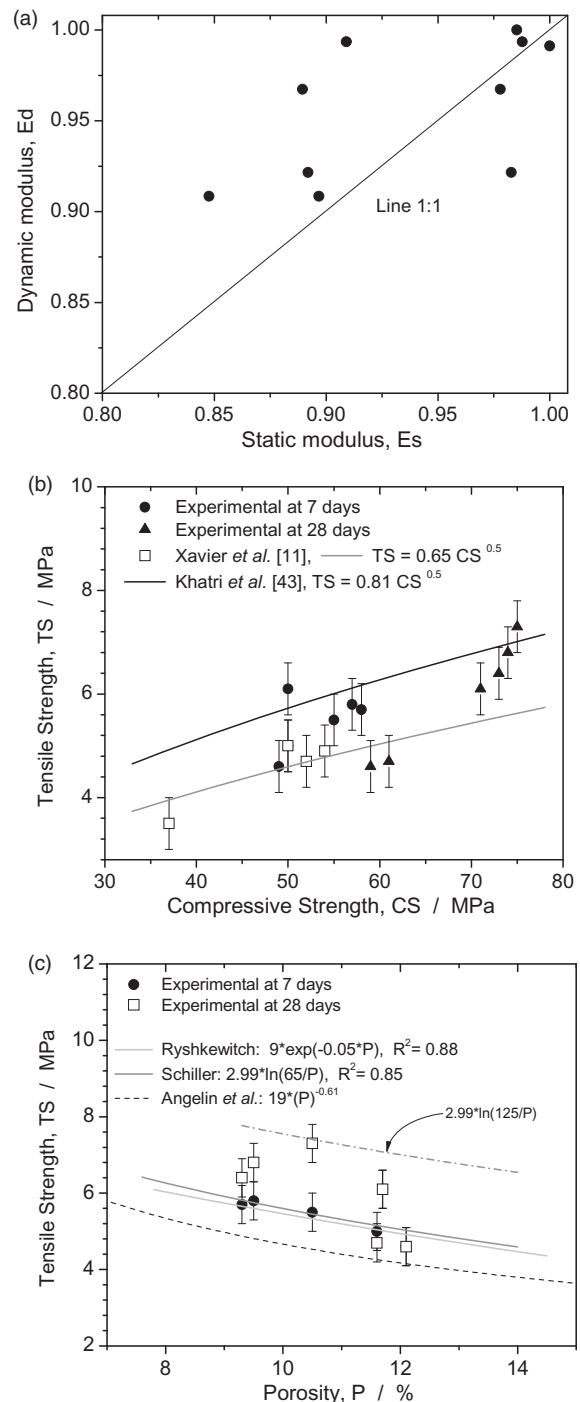
combination of material variability and the influence of the method adopted. It is recognized that a dynamic method commonly offers most accurate measurements due to the simple geometry and test set-up.<sup>42</sup> When IET (non-destructive method) is applied, the effects of voids are suppressed when the destructive method (static) is compared. Very low level of stress is applied when IET is carried out. Thus, no microcracks and the creep effect are not provided. The mentioned method is intimately associated with elastic behavior of the material. This is similar to that mentioned tangent method.<sup>42,43</sup> This reveals that this method has some advantages when compared with the static method. A non-destructive test has reproducibility in short-period using the same sample. Since a lower amount of samples is required, a lower susceptibility to experimental errors due to the number of variables is provided.<sup>43</sup>

Figure 2(a) shows a relation between the dimensionless IET (dynamic method) and compressive (static method) and the elastic moduli of the examined samples, as also carried out by Norambuena-Contreras et al.<sup>44</sup> In order to facilitate the comparison between  $E_d$  (IET method) and  $E_s$  (compressive method) results, the moduli are normalized (between 0 and 1), as previously suggested.<sup>44</sup> For this purpose, each one of the modulus is divided by the maximum of each corresponding data series. Although the dynamic and static moduli are physically correlated,<sup>45</sup> depending of the aggregate size and distinct additions (e.g. rubber particles, fibers, etc.), it is known that distinct ITZs (interfacial transition zones) and consequently microcrack widths are created.

Depending of the nature and aspect of the ITZ, the mechanical property is positive or negatively affected. When HESF and coarse aggregates are used, ITZs are created and the elasticity moduli based on static (compressive method) and dynamic (IET method) provide slight different values. This indicates that a correlation between  $E_d$  and  $E_s$  is not provided, as also reported by Norambuena-Contreras et al.<sup>44</sup> This suggests that inside the samples, a random fiber distribution is potentially constituted.<sup>44,45</sup>

Figure 2(b) shows the correlation evidencing an exponential dependence of the tensile property with compressive strength (expressed by  $TS = k CS^{0.5}$ ). Angelin et al.,<sup>39</sup> Khatri et al.,<sup>46</sup> Ramli and Dawood<sup>47</sup> and Xavier et al.<sup>11</sup> have reported similar correlations when rubber, furnace slag/fly ash, flowable high strength mortar and MG contents are utilized, respectively.

The equations proposed by Xavier et al.<sup>11</sup> and Khatri et al.<sup>46</sup> delimitate the upper and lower limits of both the experimental results at 7 and 28 days, as depicted in Figure 2(b). When the TS is correlated with porosity (or void index), exponential and logarithmic



**Figure 2.** (a) Relation between the dimensionless IET (dynamic method) and compressive (static method) and the elastic moduli of the SCC samples examined; (b) correlation describing  $TS = k CS^{0.5}$ ; (c) exponential and logarithmic equations accordingly to Ryshkewitch' and Schiller's models.

equations are similar when Ryshkewitch' and Schiller's models are considered, as also previously reported.<sup>11,39</sup> These models correlate  $k$  and  $n$  as empirical constant and  $P_0$  and  $CS_0$  representing porosity level at zero



**Table 5.** Experimental results of water absorption, voids index, specific mass and specific strengths of the proposed distinct SCC samples.

Mixtures	Water absorption (%)	Voids index (%)	Specific mass (kg/m <sup>3</sup> )	Specific strength <sup>a</sup> (103 × m <sup>2</sup> s <sup>-2</sup> )		Specific strength <sup>b</sup> (103 × m <sup>2</sup> s <sup>-2</sup> )	
				at 7 days	at 28 days	at 7 days	at 28 days
SCC	5.1 (±0.5)	12.1 (±0.5)	2,370 (±0.01)	20.7 (±0.2)	24.9 (±0.2)	1.94 (±0.2)	1.95 (±0.2)
SCC/20MG	4.9 (±0.4)	11.6 (±0.5)	2,370 (±0.01)	21.1 (±0.2)	26.2 (±0.2)	1.99 (±0.2)	2.11 (±0.2)
SCC/10SF	<b>4.0 (±0.3)</b>	<b>9.3 (±0.4)</b>	2,320 (±0.01)	<b>25.9 (±0.2)</b>	<b>31.8 (±0.2)</b>	2.46 (±0.2)	<b>2.76 (±0.2)</b>
SCC/30MG/10SF	<b>4.1 (±0.4)</b>	<b>9.5 (±0.4)</b>	2,340 (±0.01)	<b>24.8 (±0.2)</b>	<b>31.6 (±0.2)</b>	<b>2.49 (±0.2)</b>	<b>2.91 (±0.2)</b>
SCC/0MG/20SF	5.0 (±0.5)	11.7 (±0.5)	2,319 (±0.01)	21.6 (±0.2)	31.4 (±0.2)	<b>2.64 (±0.2)</b>	2.66 (±0.2)
SCC/30MG/20SF	4.5 (±0.6)	10.5 (±0.5)	2,306 (±0.01)	24.3 (±0.2)	<b>32.1 (±0.2)</b>	2.39 (±0.2)	<b>3.17 (±0.2)</b>

<sup>a</sup>Specific strength determined using CS values (Table 3) per specific mass.

<sup>b</sup>Specific strength determined using TS values (Table 3) per specific mass.

strength and compressive strength at zero porosity, as shown in Figure 2(c).

Interestingly Schiller's equation describes the experimental results of the examined SCC with both MG and HESF samples when 7 day of curing is considered. When the experimental results of 28 days are considered, the Schiller's equation is modified and an upper limit is determined. Thus, the results of 28 days are scattered between the equations proposed by Angelin et al.<sup>39</sup> and the modified Schiller's equation ( $2.99 \cdot \ln(125/P)$ ).

The experimental results of the water absorption (WA), voids index (VI), specific mass (SM) and specific strengths (SS) of the examined SCC samples are shown in Table 5. Although a same order of magnitude of the WA results is attained, it is observed that the two lowest values are those corresponding with the SCC/10SF and SCC/30MG/10SF samples. Besides, these two same SCC samples have demonstrated the two lowest voids index (porosity) values, which have reached up to 30% lower than other samples examined.

These aforementioned results seems to be associated with slight silica fume contents, which are absence in other mixtures examined. When the efficiency factors or specific strengths (SS) are determined (*i.e.* CS per SM and TS per SM),<sup>11,39,40</sup> the highest SS values are those of the SCC/30MG/20SF samples. However, both the SCC/10SF and the SCC/30MG/10SF samples have exhibited similar SS values. As previously commented, the SCC/30MG/10SF and SCC/10SF samples have also demonstrated the best results in terms of the CS and TS results associated with very acceptable L-box results (workability).

Figure 3(a) and (b) demonstrates the experimental results of the CS as a function of the porosity considering both the results of curing at 7 and 28 days, respectively. Figure 3(a) shows a modified Ryshkewitch's equation (*i.e.*  $128 \cdot e^{(-0.082 \cdot P)}$ ) the CS = f(P) for the

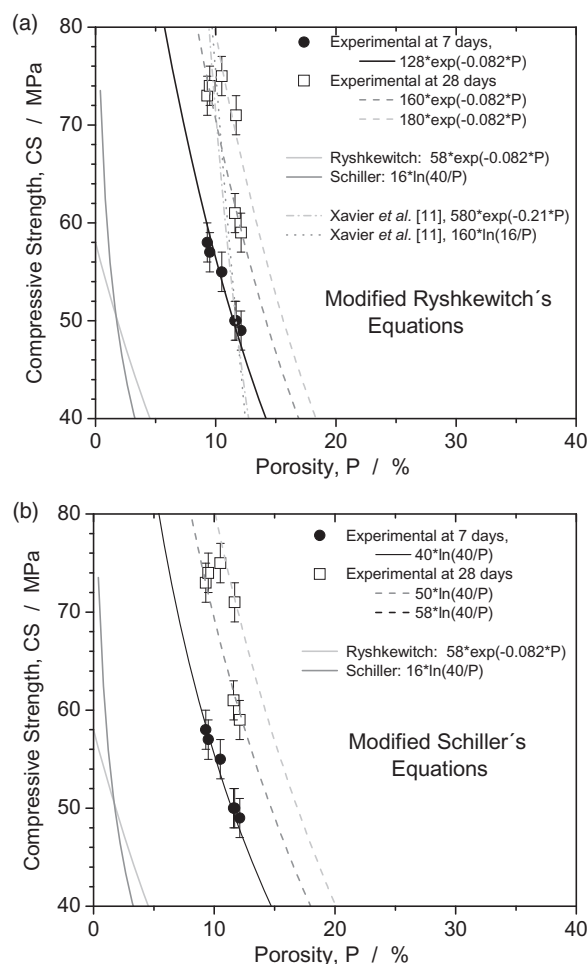


**Figure 3.** Modified Ryshkewitch's (a) and Schiller's (b) equations describing compressive strength (CS) as a function of porosity (P), *i.e.* CS = f(P), for the experimental results at 7 and 28 days.

experimental results at 7 days. It is observed that the equations proposed by Xavier et al.<sup>11</sup> indicate another inclinations not agreeing with experimental results attained.

Additionally, when the results obtained at 28 days of curing, only one kind of equation is enough to prescribe the attained results. Thus, a range with two modified Ryshkewitch's equations describes the dispersion observed, *i.e.* between 160 and 180  $e^{(-0.082 P)}$ . Interesting that only the constant is modified, which is increased when the results of 7 and 28 days are compared. When the modified Schiller's equations are analyzed, analogue modifications are also occurred, as shown in Figure 3(b). The results at 7 days indicate that the results CS are modified, *i.e.*  $40 \ln(40/P)$ . On the other hand, two equations are used in order to prescribe the dispersion range (at 28 days), *i.e.* 50 and  $58 \ln(40/P)$ . It can be observed that only the constant is modified. The correlations between the SS as a function of the examined porosity considering the curing days of 7 and 28 days are shown Figure 4(a) and (b). Both the modified Ryshkewitch's equations and those proposed by Xavier et al.<sup>11</sup> are shown in Figure 4(a). Although the equations proposed by Xavier et al.<sup>11</sup> considering both Ryshkewitch' and Schiller's models are also plotted in Figure 4(a), it is revealed that the original Ryshkewitch's model exhibits modification only into the constant. Thus, the experimental results of both 7 and 28 days are better fitted, *i.e.*  $56 e^{(-0.082 P)}$ , with  $R^2=98\%$  and  $68 e^{(-0.082 P)}$  with  $R^2=82\%$ , respectively.

Figure 4(b) shows the modified Schiller's models (considering SS *vs.* porosity) varying only the constants. The experimental results of the curing at 7 and 28 days are described by  $18 \ln(40/P)^{(-0.082 P)}$ , with  $R^2=99\%$  and  $70 \ln(40/P)$  with  $R^2=78\%$ , respectively. Once again, it is remarked that those equations proposed by Xavier et al.<sup>11</sup> are compared due to the modified SCC with distinct MG contents are used. It is worth noted that, in this current study, the SCC samples are prepared by using only MG and HESF contents. Also, it is remembered that similar w/c ratio and HES cement is utilized. This slightly increases the CS result attained when investigations utilizing OPC<sup>45-48</sup> or containing rubber contents are compared.<sup>39</sup>

### SEM observations and MG and HESF content correlations

Figure 5(a) and (b) shows the resulting microstructures of the examined SCC samples in two distinctive magnifications. A region designated as ITZ ( $\sim 9 \mu\text{m}$ ) is constituted. This is characterized between C-S-H and gravel. When the resulting microstructural array of SCC/20MG sample is analyzed, formation characterizing CH (calcium hydroxide, Portlandite) and C-S-H (calcium silicate hydrated) are identified, as depicted in Figure 5(c) and (d). It is previously reported<sup>11</sup> that MG addition has provided higher portions of both the

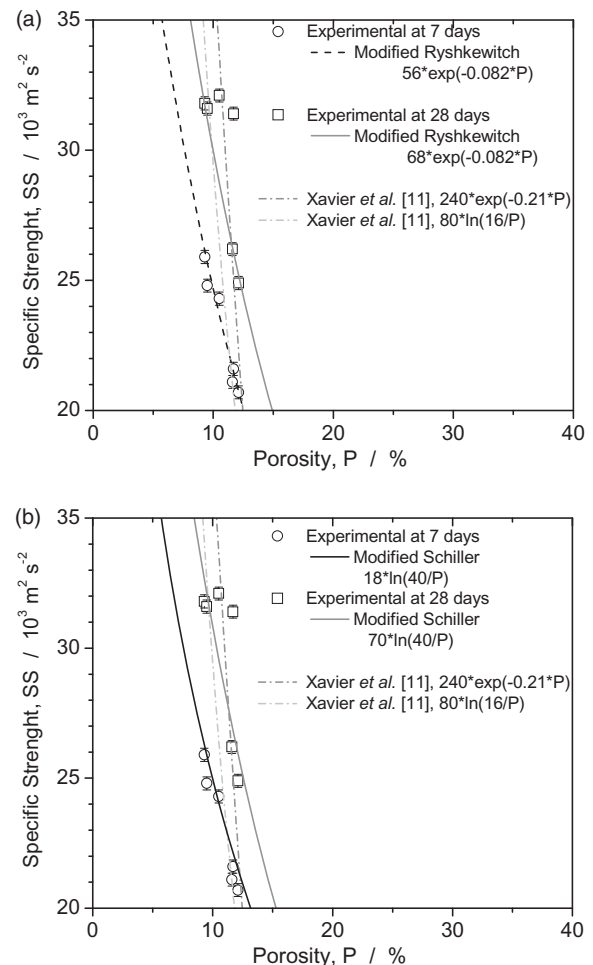


**Figure 4.** Modified Ryshkewitch's (a) and Schiller's (b) equations describing specific strength (SS) as a function of porosity (P), *i.e.*  $SS = f(P)$ , for the experimental results at 7 and 28 days.

CH and C-S-H in a SSC modified with MG content than in a conventional SCC sample. Also, the region prescribing the ITZ between mainly C-S-H and gravel is clearly characterized. Similarly to the SCC samples examined, at the region of the ITZ the microcracks with width of about  $9 (\pm 0.85) \mu\text{m}$  are characterized.

Figure 5(e) and (f) shows the microstructures of the SCC/10SF sample. Although steel fibers are not exhibited in these two SEM magnifications, the region delimitating the ITZ constituted between C-S-H and gravel is demonstrated. Considering the SCC/10SF sample, the average of the widths of the microcracks surrounding the ITZ is of about  $9 (\pm 0.85) \mu\text{m}$ .

The embedded HESF (with a diameter  $\sim 0.55 \text{ mm}$ ) images corresponding with two magnifications of the SCC/30MG/10SF sample are shown in Figure 6(a) and (b). This SEM image is representative for all other embedded HESF SCC samples. A very good adherence of the HESF with cement paste is clearly evidenced, as

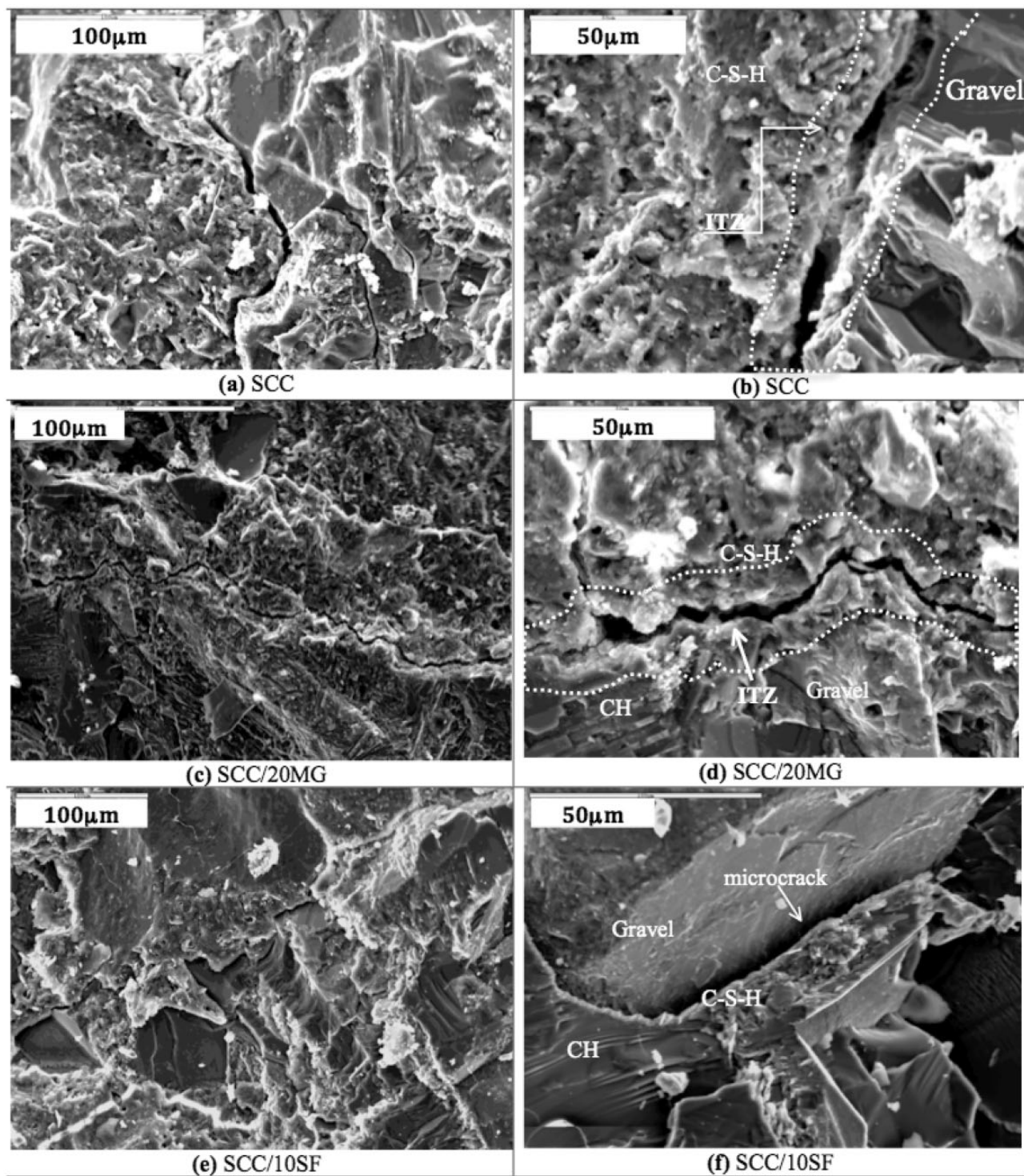


**Figure 5.** Typical resulting microstructural arrays of the examined SCC samples of: (a) and (b) SCC mixture sample, (c) and (d) SCC/20MG sample, and (e) and (f) SCC/10SF sample evidencing the region delimitating the ITZ between C-S-H and gravel.

previously reported.<sup>49</sup> This indicates that a “strong” bond between oxidation products (rust) on the fiber’s surface and cement paste (C-S-H). The rust produced on surface of the HESF contains small pores and water can be incorporated. When the hydration stage is

occurring, the tricalcium aluminate  $C_3A$  ( $CaO \cdot Al_2O_3$ ) phase is hydrated (*i.e.*  $CaO \cdot Al_2O_3 \cdot xH_2O$ ), and it reacts with ions on surface of the embedded HESF. Considering a steel bar immersed in water, commonly  $Fe(OH)_2$  is produced. With the oxidation evolution, a



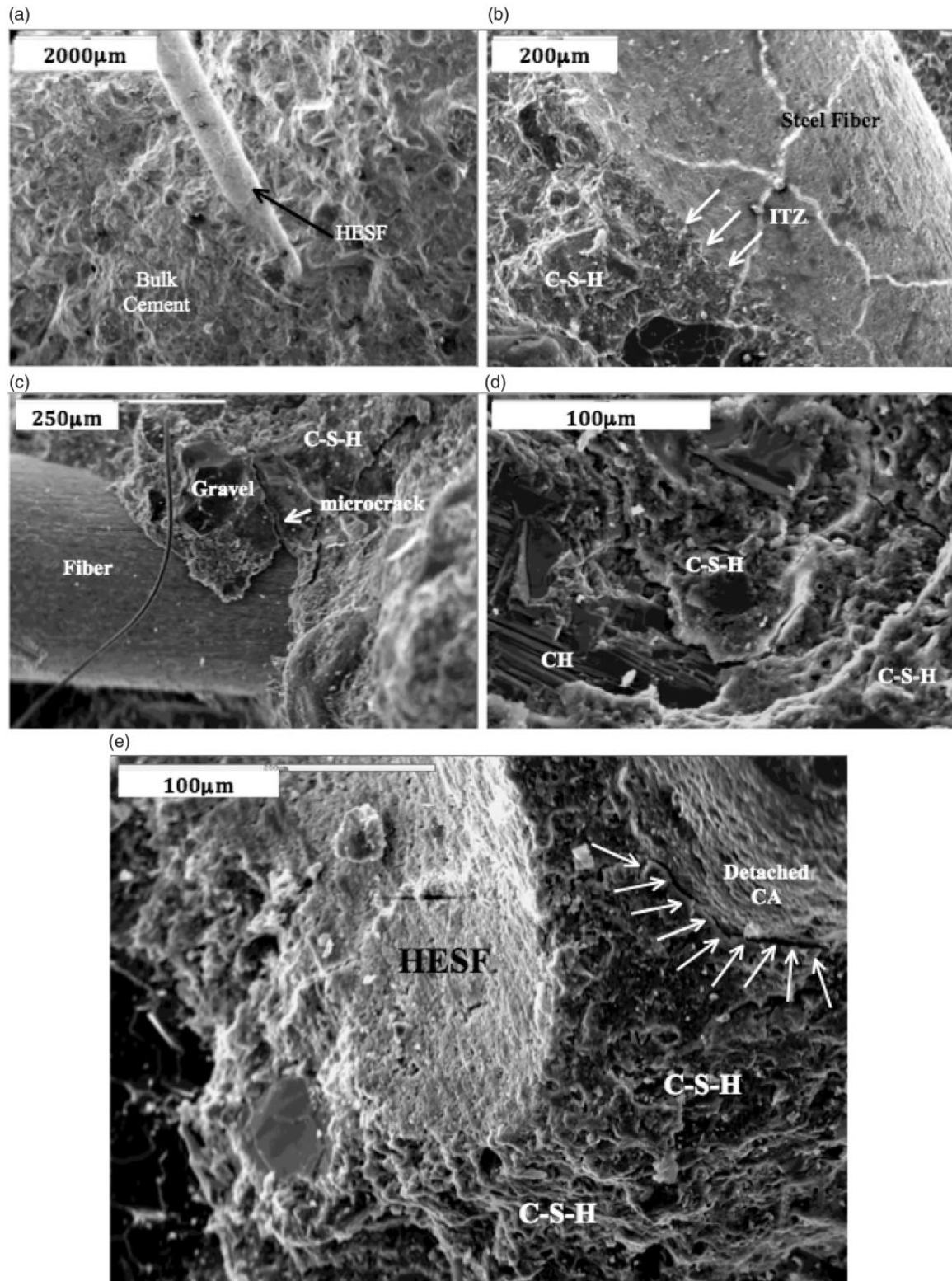


**Figure 6.** Typical hook-end steel fiber (HESF, Dramix® 3 D with diameter  $\sim 0.55$  mm) corresponding with the SCC/30MG/10SF sample (a) and (b) evidencing a good bonding between HESF and cement paste; (c) certain loss of adherence of the HESF with cement matrix and the micro cracking formation delimitating both CH and C-S-H phases are shown; (d) micrograph evidencing both CH and C-S-H formation in a SCC/30MG/20SF sample; and (e) SEM image showing interface between the HESF and cement paste and decreased microcracks ( $\leq 5 \mu\text{m}$ ) between coarse aggregate (CA) and cement paste.



**Table 6.** Relative values of SS at 7 and 28 days, consumption of cement (CC) and its relative value, and relative values of CC per SS and consumptions of cement per compressive strength (CS) at 28 days.

Mixtures	Relative SS <sup>a</sup> at 7d 28d		Relative SS <sup>b</sup> at 7d 28d		Consumption cement (CC) (kg/m <sup>3</sup> )	Relative CC	Relative CC/SS <sup>c</sup>	CC/CS (kg.m <sup>-3</sup> .MPa <sup>-1</sup> ) <sup>d</sup>
SCC	1	1	1	1	380	1	1	6.44
SCC/20MG	1.02	1.05	1.09	1.02	369	0.971	0.95	6.05
SCC/10SF	1.25	1.28	1.27	1.42	367	0.965	0.68	5.03
SCC/30MG/10SF	1.20	1.27	1.28	1.50	367	0.965	<b>0.64</b>	<b>5.03</b>
SCC/0MG/20SF	1.04	1.26	1.36	1.36	365	0.961	0.71	5.14
SCC/30MG/20SF	1.17	1.29	1.23	1.63	350	0.921	<b>0.57</b>	<b>4.79</b>

<sup>a</sup>Values with respect to CS values in Table 5.<sup>b</sup>Values with respect to TS values in Table 5.<sup>c</sup>Values with respect to relative CC per SS<sup>(\*)</sup> considering 28 days.<sup>d</sup>Values with respect to CC per CS (Table 3) considering 28 days, based on literature.<sup>51</sup>

compound  $\text{Fe}(\text{OH})_3$  is provided, and specimens link  $\text{Fe}_2\text{O}_3 \cdot x\text{H}_2\text{O}$  can be produced. When hydrated  $\text{CaO}$ ,  $\text{Al}_2\text{O}_3$  is involved with (or reacting)  $\text{Fe}(\text{OH})_2 \cdot x\text{H}_2\text{O}$  or with some one modified iron hydroxide specie, a possible molecular affinity (species similarity) seems to contribute with a “strong” bonding between HESF and cement paste. This corroborates with the substantial decreasing of the ITZ formation (or its absence) when the cement paste is cured.

Figure 6(c) and (d) shows the resulting loss of adherence of the embedded HESF with cement matrix. The formation of both CH and C-S-H is also depicted. This means that the absence of the MG content (which induces to better workability up to certain limit content<sup>11</sup>) provokes certain weakness in the adherence between the HESF and cement paste, as shown in Figure 6(c). This consequently affects the mechanical behavior. When the SCC/10SF sample (without MG content) is compared with the SCC/30MG/10SF sample, it clearly observed that their corresponding compressive strengths (at 7 and 28 days) are very similar, as shown in Table 3. On the other hand, when the flexural (tensile) characteristic is considered, which is affected by the embedded HESF, it is slightly observed that the samples containing MG content (SCC/30MG/10SF) has TS value slightly higher (~6%) than the SCC/10SF sample. Also, the effect of the MG content is also observed when the SCC/30MG/10SF and SCC/0MG/20SF samples are compared (Table 3). Although the HESF content is two times higher, similar CS values are observed. Also, associated with this, a deleterious effect in the flexural characteristic is observed. The SCC/0MG/20SF sample has TS lower of about 12%, mainly at 28 days of curing. This induces that the MG content seems to contribute with adherence of steel fiber with cement matrix. Besides, an improvement in the flexural characteristic is also observed. Additionally, it is also indicated that the

MG content facilitates both CH and C-S-H formation, as depicted in Figure 6(d).

A detail evidencing the interface between the HESF and cement paste is depicted in Figure 6(e). This suggests a stronger bonding than the sample without MG content. When a CA (coarse aggregate) is detached, a region defining the ITZ ( $\leq 5 \mu\text{m}$ ) with cement paste seems to be reasonably lower (2 times) than the SCC without MG content. This corroborates with the hypothesis assumed that the MG content improves the workability and the resulting bonding of both HESF and CA particles, as shown in Figure 6(e).

In all examined microstructures of the SCC samples, no ettringite formations are characterized. It is known that these species provide expansion and disruption of the cement, and consequently, the mechanical behavior is decreased.<sup>11,50</sup> Based on this, it seems that C-S-H and HESF content are responsible for the resulting mechanical properties, contributing with CS and TS results.

Another important parameter when planning a SCC is the cement consumption (CC). This directly reflects in the relative concrete costs. From those six distinct SCC mixture samples used in this current investigation, the highest cement consumption (CC) utilized is that of the SCC mixture (*i.e.* 380 kg/m<sup>3</sup>). This is followed by the SCC/20MG, the SCC/10SF and the SCC/30MG/10SF samples with CC values of 369, 367 and 367 kg/m<sup>3</sup>, respectively. The two lowest CC values are those corresponding with the SCC/0MG/20SF and SCC/30MG/20SF samples, as demonstrated in Table 6. Remembering that a SS parameter demonstrates mechanical behavior concatenated with lightweight effect. Although it is recognized that a lightweight effect is not an intrinsic characteristic required for a SCC mixture, these values of CC/SS are compared, as shown in Table 6.

When the ratios between the relative values (at 28 days) of CC and specific strengths (SS) are compared, the two lowest CC per SS values are those corresponding of the SCC/30MG/10SF and the SCC/30MG/20SF samples. The cement consumption per compressive strength (CC/CS) at 28 days is another important parameter to be considered, as previously reported by Damineli et al.<sup>51</sup> They have reported at least 40 distinctive published articles concerning to Brazilian and international data of cement consumption per compressive strength, and different mix design methods are also considered. Based on analysis of CC per CS, they have suggested that in future, a cement consumption of  $5 \text{ kg m}^{-3} \text{ MPa}^{-1}$  is a feasible goal for normal strength ( $< 50 \text{ MPa}$ ) concrete. With this assertion, the obtained results in this current study of the CC per CS are also included in Table 6. Interestingly, from the six proposed SCC mixtures, three are very close to that of value suggested of  $5 \text{ kg m}^{-3} \text{ MPa}^{-1}$ , which is indicated by Damineli et al.<sup>51</sup> Additionally, it is remarked that the SCC samples containing both MG and HESF contents are inside of the mentioned CC per CS range.

Figure 7 shows a representation of the relation between CC/CS per CS proposed by Damineli et al.<sup>51</sup> In this representation, the attained results in this investigation are also plotted. The two blacked-circles are representing the SCC and SCC/20MG samples. Other three open circles are four distinct mixtures due to two results are overlapped, as can be seen in Table 6. It is noticeable that the open circles are located at region indicating low cement consumption. Also, the

dispersion of the results decreases with the increase of the compressive strength, as also previously reported.<sup>51</sup>

Based on the fact the porosity (P) (former designated as void index) has also an important role in the mechanical responses of the SCC sample, the parameter “P” is also related with the CC for all samples examined, as shown in Table 7. Evidently, those samples with lower P levels exhibit lower P/CC ratios than other samples examined, *i.e.* the SCC/10SF and SCC/30MG/10SF. It is also considered that a parameter correlating the porosity level (P) per cement consumption (CC) associated with mechanical behavior constitutes another important role to contribute in the design of mixtures. Thus, both the parameters P/C/Cs and P/CC/TS suggest that the SCC/30MG/10SF and the SCC/10SF samples are interesting attractive.

When the SCC samples containing only HESF content are compared, *i.e.* the SCC/10SF and the SCC/0MG/20SF samples, the parameters PP/CC/CS and PP/CC/TS indicate that the increase of the HESF content (*i.e.*  $10 \text{ kg/m}^3$  to  $20 \text{ kg/m}^3$ ) has also increased ( $\sim 30\%$ ) these parameters, *i.e.* from 0.35. to  $0.45 \times 10^3 \text{ m}^{-3} \text{ kg}^{-1} \text{ MPa}^{-1}$ , and from  $3.96$  to  $5.25 \times 10^3 \text{ m}^{-3} \text{ kg}^{-1} \text{ MPa}^{-1}$ , respectively. This means that increasing the HESF content, a worst behavior is provided.

When the MG and HESF contents are considered, the SCC/30MG/10SF sample reveals the lowest PP/CC/TS, mainly due to the flexural characteristic is taken in account. With this, analyzing all proposed parameters, considering mechanical resistance concatenated with light weight effect, lower cement consumption, lower steel fiber content and porosity

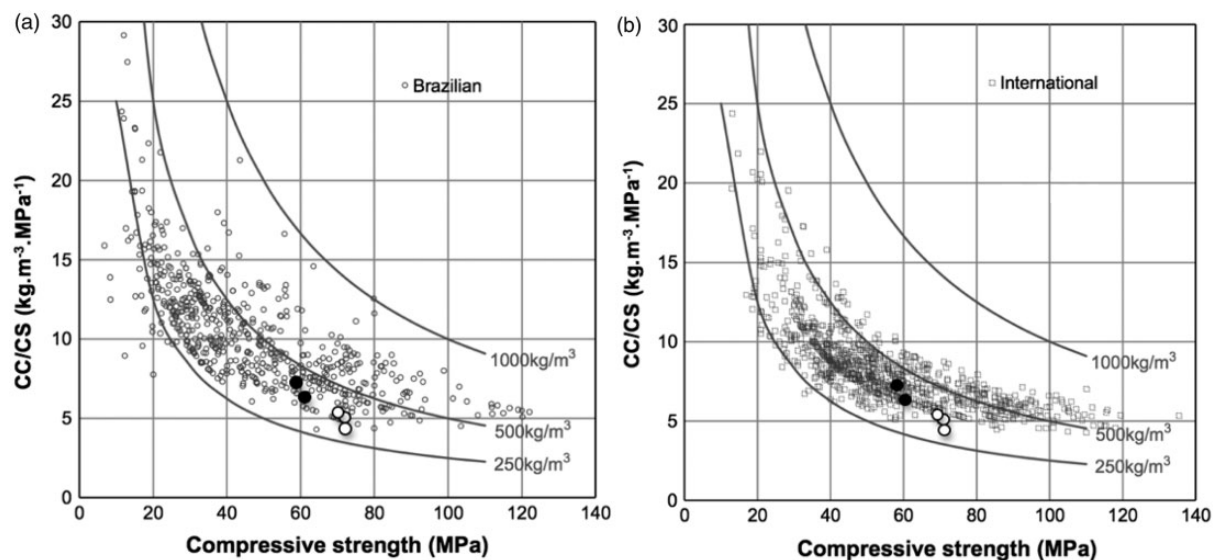


**Figure 7.** Relation between CC/CS per CS proposed by Damineli et al.<sup>51</sup> with Brazilian results (a) and international results (b) including the experimental data from this investigation.

**Table 7.** Comparisons of amount of porosity (P) per consumption of cement (CC), and its relation with both the compressive (CS) and tensile (TS) strengths at 28 days for all examined SCC mixture samples.

Mixtures	Porosity (P) per CC ( $10^3 \times \text{m}^{-3} \text{ kg}^{-1}$ )	P/CC/CS <sup>a</sup> ( $10^3 \times \text{m}^{-3} \text{ kg}^{-1} \text{ MPa}^{-1}$ )	P/CC/TS <sup>b</sup> ( $10^3 \times \text{m}^{-3} \text{ kg}^{-1} \text{ MPa}^{-1}$ )
SCC	0.32	0.54	6.92
SCC/20MG	0.31	0.52	6.69
SCC/10SF	<b>0.25</b>	<b>0.35</b>	<b>3.96</b>
SCC/30MG/10SF	<b>0.26</b>	<b>0.36</b>	<b>3.81</b>
SCC/0MG/20SF	0.32	0.45	5.25
SCC/30MG/20SF	0.30	0.41	4.11

<sup>a</sup>Values with respect to CS values at 28 days.<sup>b</sup>Values with respect to TS values at 28 days.

level, the SCC/30MG/10SF sample exhibits the promising indicators to be adopted in mixture designing.

## Conclusions

From the experimental results concerning to fresh and hardened properties of six distinct self-compacting concrete and associating with important parameters to mixture design, the following conclusions can be drawn:

- The adopted mixtures demonstrate satisfactory workability accordingly with international standard for a self-compacting concrete. Additionally, the MG content reveals that SCC characteristic is attained. Compared with the conventional SCC mixture, it is found that compressive strength (CS) at 7 days is not substantially increased when only steel fibers are added. On the other hand, when the CS results at 28 days are analyzed, all SCC samples with fibers have exhibited similar CS. When the tensile strength (TS) results at 7 days of curing are analyzed, all samples with steel fibers revealed of about 30% higher than other examined samples. At 28 days, this difference has increased (~60%).
- When both mechanical strength and lightweight effect are concatenated, the specific strength (SS) parameters indicate the highest values are those of the SCC/10SF and the SCC/30MG/10SF samples. Considering the SS values based on the CS values at 28 days, the SCC/30MG/10SF sample has its corresponding SS up to 27% higher than the SCC sample, and up to 50% higher than the SCC sample, when the SS is calculated considering at 28 days and TS values.
- When the cement consumption (CC) per CS at 28 days is analyzed, the SCC/30MG/10SF samples also exhibits a competitive value, (*i.e.*  $\sim 5 \text{ kg} \cdot \text{m}^{-3} \cdot \text{MPa}^{-1}$ ), which means of about 30% lower than the SCC sample. Additionally, when the parameter

considering porosity level per cement consumption, also associated with mechanical behavior (per CS and per TS strengths), the SCC/30MG/10SF sample also indicates the best performance.

## Data availability

The authors declare that all research data supporting this publication are directly available within this publication.


## Declaration of Conflicting Interests

The author(s) declared no potential conflicts of interest with respect to the research, authorship, and/or publication of this article.

## Funding

The author(s) disclosed receipt of the following financial support for the research, authorship, and/or publication of this article: This study was funded by the FAEPEX-UNICAMP (#2317/20), CAPES (Coordination for the Improvement of Higher Education Personnel, Ministry of Education, Brazil, Grant #1), CNPq (The Brazilian Research Council) Grants #311009/2017-4; # 406234/2018-3; #309409/2017-9 and #304950/2017-3, #405602/2018-9.

## ORCID iDs

Mirian LNM Melo  <https://orcid.org/0000-0001-9668-7799>  
 Wislei R Osório  <https://orcid.org/0000-0002-2754-9584>

## References

1. Zheng X, Zhang J and Wang Z. Effect of multiple matrix cracking on crack bridging of fiber reinforced engineered cementitious composite. *J Compos Mater* 2020; 54: 3949–3965.
2. Cao Q, Lv X, Li X, et al. High strength expansive concrete-encased-steel filled carbon fiber reinforced polymer tubes under axial monotonic and cyclic load. *J Compos Mater* 2020; 54: 4557–4573.
3. Okamura H and Ouchi M. Self-compacting concrete. *ACT* 2003; 1: 5–15.

4. EFNARC. The European Guidelines for self-compacting concrete - specification, production and use. *Eur Fed Spec Constr Chem Concr Syst* 2005; 63.
5. Hammeed A, Qazi A, Abbas S, et al. Self-compacting concrete: use of waste marble powder as filler material. *Pak J Eng Appl Sci* 2016; 18: 1–10.
6. Devi R, Tej S and Kumar SN. Experimental investigation on self compaction concrete using marble dust as partial replacement to cement. *Int J Scient Res Dev* 2017; 5: 338–341.
7. Moretti JP, Nunes S and Sales A. Self-compacting concrete incorporating sugarcane bagasse ash. *Constr Build Mater* 2018; 172: 635–649.
8. Nguyen HA, Chang TP, Shih JY, et al. Enhancement of low-cement self-compacting concrete with dolomite powder. *Constr Build Mater* 2018; 161: 539–546.
9. Kannan V. Strength and durability performance of self-compacting concrete containing self-combusted rice husk ash and metakaolin. *Constr Build Mater* 2018; 160: 169–179.
10. Singh N and Singh SP. Evaluating the performance of self compacting concretes made with recycled coarse and fine aggregates using non destructive testing techniques. *Constr Build Mater* 2018; 181: 73–84.
11. Xavier BC, Verzegnassi E, Bortolozzo AD, et al. Fresh and hardened states of distinctive self-compacting concrete with marble- and phyllite-powder aggregate contents. *J Mater Civ Eng* 2020; 32: 04020065.
12. Tomar AK, Gupta SK, Kumar A, et al. Review on utilization of waste marble powder in self-compacting concrete. *Int J Eng Trends Technol* 2016; 37: 122–124.
13. Tayeb B, Abdelbaki B and Madani ML. Effect of marble powder on the properties of self-compacting sand concrete. *Open Constr Build Technol J* 2011; 5: 25–29.
14. Singh M, Choudhary K, Srivastava A, et al. A study on environmental and economic impacts of using waste marble powder in concrete. *J Build Eng* 2017; 13: 87–95.
15. Kabeer KISA and Vyas AK. Utilization of marble powder as fine aggregate in mortar mixes. *Constr Build Mater* 2018; 165: 321–332.
16. Toubal Seghir N, Mellas M, Sadowski L, et al. Effects of marble powder on the properties of the air-cured blended cement paste. *J Cleaner Prod* 2018; 183: 858–868.
17. Belaidi ASE, Azzouz L, Kadri E, et al. Effect of natural pozzolana and marble powder on the properties of self-compacting concrete. *Constr Build Mater* 2012; 31: 251–257.
18. Tunc ET. Recycling of marble waste: a review based on strength of concrete containing marble waste. *J Environ Manag* 2019; 231: 86–97.
19. Alberti MG, Enfedaque A and Gálvez JC. The effect of fibres in the rheology of self-compacting concrete. *Constr Build Mater* 2019; 219: 144–153.
20. Zhang P, Zheng Y, Wang K, et al. Combined influence of nano-CaCO<sub>3</sub> and polyvinyl alcohol fibers on fresh and mechanical performance of concrete incorporating fly ash. *Struct Concr* 2020; 21: 724–734.
21. Zhang P, Li Q, Chen YZ, et al. Durability of steel fiber-reinforced concrete containing SiO<sub>2</sub> nano-particles. *Materials* 2019; 12: 2184.
22. Zhang P and Li QF. Effect of polypropylene fiber on durability of concrete composite containing fly ash and silica fume. *Compos Part B: Eng* 2013; 45: 1587–1594.
23. Murugan RB, Haridharan MK, Natarajan C, et al. Influence of glass fiber on fresh and hardened properties of self compacting concrete. *IOP Conf Ser: Earth Environ Sci* 2017; 80: 012004.
24. Bhaskar R, Nallanathel M, Gokulnath V, et al. Influence of m-sand on the compressive strength of M-30 grade polypropylene fiber-reinforced SCC. *Inter J Pure Appl Mater* 2018; 119: 17.
25. Bordelon AC and Roesler JR. Spatial distribution of synthetic fibers in concrete with X-ray computed tomography. *Cem Concr Compos* 2014; 53: 35–43.
26. Li VC, Wang Y and Backer S. A micromechanical model of tension-softening and bridging toughening of short random fiber reinforced brittle matrix composites. *J Mech Phys Solids* 1991; 39: 607–625.
27. Geng YP and Leung CKY. Micromechanics-based FEM simulation of fiber-reinforced cementitious composite components. *Comput Struct* 1997; 64: 973–982.
28. Torrijos MC, Barragán BE and Zerbino RL. Placing conditions, mesostructural characteristics and post-cracking response of fibre reinforced self-compacting concretes. *Constr Build Mater* 2010; 24: 1078–1085.
29. Ghasemi M, Ghasemi MR and Mousavi SR. Studying the fracture parameters and size effect of steel fiber-reinforced self-compacting concrete. *Constr Build Mater* 2019; 201: 447–460.
30. Abdallah S, Rees DWA, Ghaffar SH, et al. Understanding the effects of hooked-end steel fibre geometry on the uniaxial tensile behaviour of self-compacting concrete. *Constr Build Mater* 2018; 178: 484–494.
31. Ananda F, Febriani O, Pribadi JA, et al. Effect the used of steel fibers (Dramix) on reinforced concrete slab. *J Infr Develop* 2019; 2: 183–191.
32. Aslani F, Hamidi F, Valizadeh A, et al. High-performance fibre-reinforced heavyweight self-compacting concrete: analysis of fresh and mechanical properties. *Constr Build Mater* 2020; 232: 117230.
33. ASTM A820/A820M. *Standard specification for steel fibers for fiber-reinforced concrete*. West Conshohocken, PA: ASTM, 2016.
34. ASSOCIAÇÃO BRASILEIRA DE NORMAS TÉCNICAS, NBR 5739 - Concreto - Ensaio de compressão de corpos de prova cilíndricos, Rio de Janeiro, 2018.
35. ASSOCIAÇÃO BRASILEIRA DE NORMAS TÉCNICAS, NBR 8522 - Concreto - Determinação dos módulos estáticos de elasticidade e de deformação à compressão, Rio de Janeiro, 2017.
36. ASTM C215-14. *Standard test method for fundamental transverse, longitudinal, and torsional resonant frequencies of concrete specimens*. West Conshohocken, PA: ASTM, 2014.



37. ASTM E1876-15. *Standard test method for dynamic Young's modulus, shear modulus, and Poisson's ratio by impulse excitation of vibration*. West Conshohocken, PA: ASTM, 2015.
38. ATCP, Guia de instruções de medição com o Sonelástico para amostras de concreto cilíndricas, São Carlos, [s.d.].
39. Angelin AF, Andrade MFF, Bonatti RS, et al. Effects of spheroid and fiber-like waste-tire rubbers on interrelation of strength-to-porosity in rubberized cement and mortars. *Constr Build Mater* 2015; 95: 525–536.
40. Angelin AF, Cecche Lintz RC, Osório WR, et al. Evaluation of efficiency factor of a self-compacting lightweight concrete with rubber and expanded clay contents. *Constr Build Mater* 2020; 257: 119573.
41. Lu X, Sun Q, Feng W, et al. Evaluation of dynamic modulus of elasticity of concrete using impact-echo method. *Constr Build Mater* 2013; 47: 231–239.
42. Lord JD and Morrel R. Comparison of static and dynamic methods for measuring the stiffness of high modulus steel and metal composites. *Can Metall Quart* 2014; 53: 292–299.
43. Otani LB and Pereira AHA. Estimation of the static modulus of elasticity of concrete using the impulse excitation technique. *ATCP Phys Eng* 2016; 38: 1–38.
44. Norambuena-Contreras J, Cartes A, Gonzalez-Torre I, et al. Effect of metallic waste addition on the physical and mechanical properties of cement-based mortars. *Appl Sci* 2018; 8: 929.
45. Valentini L, Parisatto M, Russo V, et al. Simulation of the hydration kinetics and elastic moduli of cement mortars by microstructural modelling. *Cem Concr Compos* 2014; 52: 54–63.
46. Khatri RP, Sirivivatnanon V and Gross W. Effect of different supplementary cementitious materials on mechanical properties of high performance concrete. *Cem Concr Res* 1995; 25: 209–220.
47. Ramli M and Dawood ET. Comparative study between flowable high strength mortar and flowing high strength concrete. *Concr Res Lett* 2011; 2: 249–261.
48. Chen X, Wu S and Zhou J. Influence of porosity on compressive and tensile strength of cement mortar. *Constr Build Mater* 2013; 40: 869–874.
49. Zhang P, Kang L, Wang J, et al. Mechanical properties and explosive spalling behavior of steel-fiber-reinforced concrete exposed to high temperature - a review. *Appl Sci* 2020; 10: 2324.
50. Marco M, Gilberto A, Tiziano C, et al. Tricalcium aluminate hydration in additivated systems. A crystallographic study by SR-XRPD. *Cem Concr Res* 2008; 38: 477–486.
51. Damineli BL, Kemeid FM, Aguiar PS, et al. Measuring the eco-efficiency of cement use. *Cem Concr Compos* 2010; 32: 555–562.